Title
On Representations for Joint Moments Using a Joint Coordinate System

Journal
Journal of Biomechanical Engineering, 135(11)

ISSN
0148-0731

Authors
O'Reilly, Oliver M
Sena, Mark P
Feeley, Brian T
et al.

Publication Date
2013-11-01

DOI
10.1115/1.4025327

Peer reviewed

A New Coordinate System for Describing Forces and Moments in the Knee Joint

Mark P. Sena
Graduate Student
UCB-UCSF Joint Program in Bioengineering
Department of Orthopaedic Surgery
University of California
San Francisco, California 94143

Brian T. Feeley
Assistant Professor in Residence
Department of Orthopaedic Surgery
University of California
San Francisco, California 94143

Jeffrey C. Lotz
Professor
Department of Orthopaedic Surgery
University of California
San Francisco, California 94143

Oliver M. O'Reilly*
Professor, Member of ASME
Department of Mechanical Engineering
University of California
Berkeley, CA 94720
oreilly@berkeley.edu

In its simplest realization, the joint formed between the femur and tibia features a pair of constraints on the relative rotation and translation of the two bones. Dating to the seminal work by Grood and Suntay [1], parameterizations of the kinematics of the knee joint which accommodate these constraints are well-known and are easy to comprehend from a clinical perspective. The purpose of the present paper is to provide an equally transparent representation of the forces and moments at the knee joint. This new representation enables a clear distinction of the constraint forces and moments acting at the knee joint from the forces and moments supplied by the ligaments and cartilage. As a result, the representation enables clearer clinical descriptions of the kinetics of the knee joint, is useful in defining stiffness matrices for the joint, and has application to helping design of total knee replacements.

1 Introduction

Motivated by anterior cruciate ligament (ACL) injuries and the 400,000 ACL reconstructions that are performed in the US each year, there is a need to characterize the stiffnesses of the knee joint. This characterization can hopefully provide one measure of a patient's susceptibility to ACL

*Corresponding author.

injury and a post-operative metric of the ACL reconstruction. These stiffness, which relate the kinematics and kinetics of the joint can also play a role in designing total knee replacements and could play a role in understanding post-operative complications, such as osteoarthritis, in ACL reconstructions.

As can be partially appreciated from Figure 1, the motion of the tibia relative to the femur is governed by the articular geometry of the knee joint which, in turn, places restrictions on possible motions. A good coordinate system is one which accommodates these restrictions and also provides easy descriptions of clinical motions. These six motions include three rotations, extension-flexion rotation, varus-valgus rotation, and internal-external rotation, and three translations, compression-distraction, lateral-medial translation, and anterior-posterior translation.[1] Seminal work by Grood and Suntay [1] provided the first coordinate system for the three-dimensional motions of the knee joint. These authors used a 1-2-3 set of Euler angles to describe the rotational motion and used the axes associated with the three individual rotations of the Euler angles to describe a set of joint translations. We denote these axes by $\{\mathbf{g}_1, \mathbf{g}_2, \mathbf{g}_3\}$ in the sequel.

After a period, Grood and Suntay's parameterizations of the kinematics of the knee joint became well-accepted. However, the corresponding developments for the kinetics were not immediately forthcoming. A primary difficulty in finding clinically relevant descriptions for the forces and moments at the knee joint can be traced to the geometry of the joint and the fact that the axes of rotation for the two of the Euler angles are not orthogonal: $\mathbf{g}_1 \not\perp \mathbf{g}_3$. Progress towards a useful representation of the forces and moments was made in 1996 by Fujie et al. [2]. Examining the paper [2] in light of the works [3–7] on dual basis vectors, we find that Fujie et al. [2] used, what is now known as, the dual Euler basis $\{\mathbf{g}^1, \mathbf{g}^2, \mathbf{g}^3\}$ to find one set of representations for these forces and moments.

The insights found in [3–7] on dual basis vectors and the role they play in the description of moments associated with rotations enables us to establish transparent representations for the forces and moments at the knee joint. Specifically, we follow [1] and use a set of 1-2-3 Euler angles to parameterize the rotation of the tibia relative to femur. This choice prescribes the set of unit vectors $\mathcal{E} = \{\mathbf{g}_1, \mathbf{g}_2, \mathbf{g}_3\}$. We then choose a related set of vectors $\mathcal{A} = \{\mathbf{a}_1, \mathbf{a}_2, \mathbf{a}_3\}$ to help parameterize the translational motion. Our choice leads to a transparent description of the tibial translations and is distinct from the two sets of vectors used in [1] to describe "joint" translations and "clinical" translations. In addition, the bases $\mathcal{A}$ and $\mathcal{E}$ are used to define a set of dual basis vectors, $\{\mathbf{a}^1, \mathbf{a}^2, \mathbf{a}^3\}$ and $\{\mathbf{g}^1, \mathbf{g}^2, \mathbf{g}^3\}$, respectively. The latter sets provide transparent representations for forces and moments. In particular, the contact force and contact moment that prevent the condyles from passing through the tibial plateau act in the $\mathbf{a}^3$ and $\mathbf{g}^2$ directions, respectively.

An outline of this paper is as follows. In Section 2.1, we discuss a range of frames associated with describing the relative motion of the tibia and femur. The background assembled in Section 2.1 is applied to the specification of a coordinate system for the knee joint in Section 3.1. Related developments for forces and moments are collected in Section 3.2, and clinical examples feature kinematics and kinetics are discussed in Section 3.4. Due to its prevalence in studies on joint kinematics, we also discuss the Jacobian associated with infinitesimal motions of the joint in Section 3.5. The paper closes in Section 4 with several comments on optimization schemes that are used to determine joint axes and a brief discussion on stiffness matrices.

For convenience, the paper has three appendices which present explicit details on several matrices and vectors that feature prominently in the paper. We also refer the interested reader to [3–5] for additional background on the dual Euler basis and its applications to conservative moments and constraint moments. The dual Euler basis is also related to the dual basis used in the screw motion descriptions of rigid body motions in [6, 7].

2 Methods

2.1 Coordinate Systems and Frames

In analysis of joints, it is standard to employ three coordinate frames: $\mathbb{L}$, $\mathbb{P}$, $\mathbb{D}$. The first of these frames, which is often known as a laboratory frame, is an inertial reference frame which is associated with a fixed point O. The second frame, is attached at a point O_P to the proximal anatomical segment and corotates with this body. Correspondingly, the third frame is attached at a point O_D to the distal anatomical segment and corotates with the distal segment. The 4 components of these respective frames are denoted by

$$\mathbb{L} = \{O, \mathbf{E}_1, \mathbf{E}_2, \mathbf{E}_3\}, \quad \mathbb{P} = \{O_P, \mathbf{p}_1, \mathbf{p}_2, \mathbf{p}_3\},$$

$$\mathbb{D} = \{O_D, \mathbf{d}_1, \mathbf{d}_2, \mathbf{d}_3\}. \tag{1}$$

Here, $\{\mathbf{E}_1, \mathbf{E}_2, \mathbf{E}_3\}$, $\{\mathbf{p}_1, \mathbf{p}_2, \mathbf{p}_3\}$, and $\{\mathbf{d}_1, \mathbf{d}_2, \mathbf{d}_3\}$ are right-handed set of orthonormal vectors.

[1] While the knee joint consists of the tibiofemoral articulation and the patellofemoral articulation, for the purposes of the present paper, attention will be focused on the former.

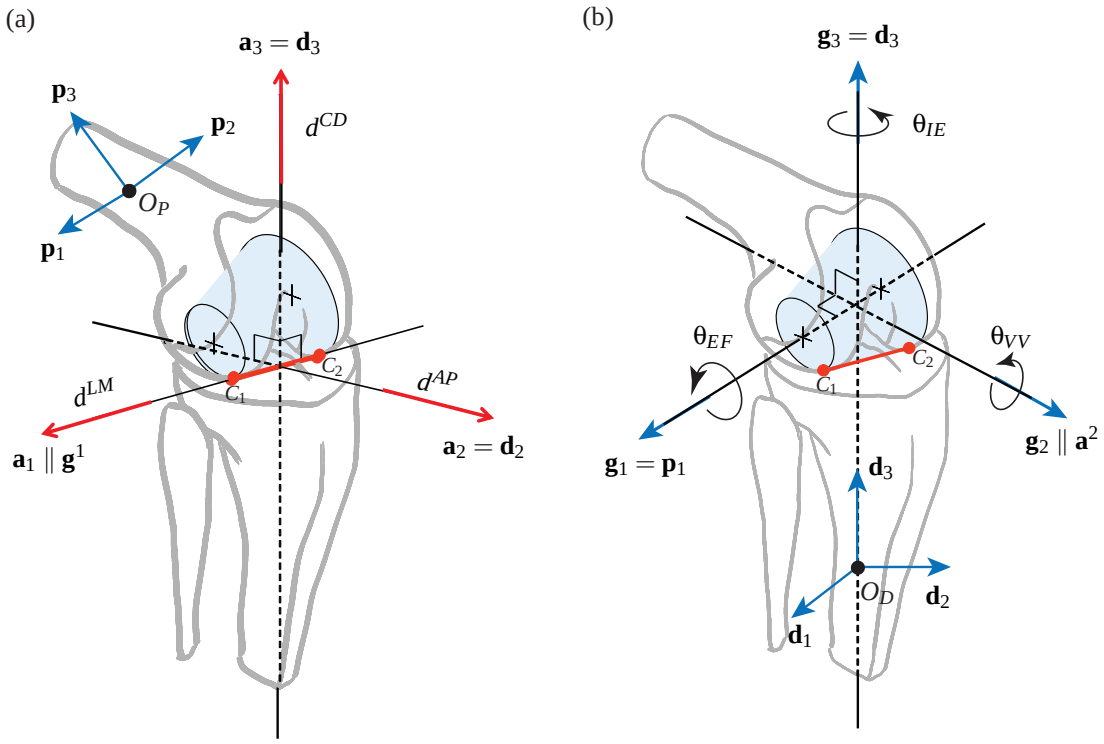

Fig. 1. Schematic of the right knee joint showing the proximal and distal frames of the femur and tibia, respectively, and a) the bases vectors $\{\mathbf{a}_1, \mathbf{a}_2, \mathbf{a}_3\}$ associated with translational motions of the knee joint and b) the bases vectors $\{\mathbf{g}_1, \mathbf{g}_2, \mathbf{g}_3\}$ associated with rotational motions of this joint. The axes are drawn to intersect in the interests of clarity.

Of particular interest is the rotation of the distal anatomical segment $\mathcal{S}_D$ with respect to the proximal anatomical segment $\mathcal{S}_P$. The rotation can be characterized by a rotation matrix R:

$$\begin{bmatrix} \mathbf{d}_1 \\ \mathbf{d}_2 \\ \mathbf{d}_3 \end{bmatrix} = \begin{bmatrix} R_{11} & R_{12} & R_{13} \\ R_{21} & R_{22} & R_{23} \\ R_{31} & R_{32} & R_{33} \end{bmatrix} \begin{bmatrix} \mathbf{p}_1 \\ \mathbf{p}_2 \\ \mathbf{p}_3 \end{bmatrix}. \tag{2}$$

Here, R_{ik} are the components of R. We also use the compact notation

$$\mathbf{d}_k = \mathsf{R}\mathbf{p}_k, \qquad (k = 1,2,3). \tag{3}$$

In the sequel, R is parameterized by a set of Euler angles ψ, θ, and ϕ. Thus, R is decomposed into the product of a rotation ψ about a unit vector $\mathbf{g}_1$ followed by a rotation θ about a unit vector $\mathbf{g}_2$ and, finally, a rotation ϕ about a unit vector $\mathbf{g}_3$. There are 12 possible sets of Euler angles, and, for each set, the first and third angles range from 0 to 2π. Depending on the specific set of Euler angles, the range of the second angle is restricted. For the 1-2-3 set of Euler angles which feature in the sequel

$$\theta \in \left(-\frac{\pi}{2}, \frac{\pi}{2}\right). \tag{4}$$

For each of the 12 sets, the three vectors $\{\mathbf{g}_1, \mathbf{g}_2, \mathbf{g}_3\}$ form a fourth set of basis vectors which is known as the Euler basis. This set of basis vectors is not orthogonal (nor is it necessarily right-handed). However, $\mathbf{g}_2$ is always perpendicular to the plane formed by $\mathbf{g}_1$ and $\mathbf{g}_3$.

A fifth set of basis vectors, which is known as the dual (or recriprocal) Euler basis $\{\mathbf{g}^1, \mathbf{g}^2, \mathbf{g}^3\}$, plays a key role in this paper. Given a specific choice of Euler angles, one is able to define the Euler basis $\{\mathbf{g}_1, \mathbf{g}_2, \mathbf{g}_3\}$. The dual Euler basis is then defined by the following 9 identities:

$$\mathbf{g}^i \cdot \mathbf{g}_k = \left\{ \begin{array}{l} 1 \text{ when } i = k \\ 0 \text{ when } i \neq k \end{array} \right\}, \qquad (i = 1,2,3, k = 1,2,3). \tag{5}$$

It is known (see, e.g., [8]) that the solutions $\mathbf{g}^i$ to these equa-

tions can be represented as follows:

$$\mathbf{g}^1 = \frac{1}{g}(\mathbf{g}_2 \times \mathbf{g}_3), \qquad \mathbf{g}^2 = \frac{1}{g}(\mathbf{g}_3 \times \mathbf{g}_1) = \mathbf{g}_2,$$

$$\mathbf{g}^3 = \frac{1}{g}(\mathbf{g}_1 \times \mathbf{g}_2). \tag{6}$$

where $g = (\mathbf{g}_1 \times \mathbf{g}_2) \cdot \mathbf{g}_3$.[2] As discussed in [4, 5], the dual Euler basis plays a key role in establishing transparent expressions for conservative moments and constraint moments. For instance, if one wishes the restrict the rotation ψ about $\mathbf{g}_3$, then a constraint moment $M\mathbf{g}^3$ needs to be applied. This moment has no components in the $\mathbf{g}_1$ or $\mathbf{g}_2$ directions and so does not affect these rotations.

The final sets of basis vectors pertain to the translational motion so a joint. We define a basis $\{\mathbf{a}_1, \mathbf{a}_2, \mathbf{a}_3\}$ which is used to describe the clinical translations of the distal segment relative the proximal segment:

$$\mathbf{u} = u^1\mathbf{a}_1 + u^2\mathbf{a}_2 + u^3\mathbf{a}_3. \tag{7}$$

This basis has a dual basis $\{\mathbf{a}^1, \mathbf{a}^2, \mathbf{a}^3\}$. The dual basis vectors are, following (5) and (6),

$$\mathbf{a}^1 = \frac{1}{a}(\mathbf{a}_2 \times \mathbf{a}_3), \quad \mathbf{a}^2 = \frac{1}{a}(\mathbf{a}_3 \times \mathbf{a}_1), \quad \mathbf{a}^3 = \frac{1}{a}(\mathbf{a}_1 \times \mathbf{a}_2), \tag{8}$$

where $a = (\mathbf{a}_1 \times \mathbf{a}_2) \cdot \mathbf{a}_3$.

A vector $\mathbf{b}$ has several distinct representations with respect to the aforementioned bases. For example,

$$\mathbf{b} = \sum_{k=1}^{3} B_k \mathbf{E}_k = \sum_{k=1}^{3} b_{p_k} \mathbf{p}_k = \sum_{k=1}^{3} b_{d_k} \mathbf{d}_k = \sum_{k=1}^{3} b^k \mathbf{g}_k = \sum_{k=1}^{3} b_k \mathbf{g}^k. \tag{9}$$

The components are obtained by projecting the vector $\mathbf{b}$ onto the appropriate basis vector. It is important to distinguish how one computes the components by projecting $\mathbf{b}$ onto the appropriate set of basis vectors. For example,

$$\mathbf{b} \cdot \mathbf{E}_k = B_k, \qquad \mathbf{b} \cdot \mathbf{g}^k = b^k, \qquad \mathbf{b} \cdot \mathbf{g}_i = b_i. \tag{10}$$

One cannot expect $b_i = b^i$. Related remarks pertain to the components of $\mathbf{b}$ along $\mathbf{a}^k$ and $\mathbf{a}_i$.

[2] For the 1-2-3 set of Euler angles used later in this paper $g = \cos(\theta)$.

3 Results

3.1 A Coordinate System for the Knee Joint

For the knee joint, we identify the proximal body with the femur and the distal body with the tibia. We follow [1] and use a set of 1-2-3 Euler angles to describe the rotation R of the tibia relative to the femur. For convenience, explicit details on the Euler and dual Euler basis vectors for this choice of Euler angles are contained in Appendix A.[3]

Three Euler angles are identified with the three rotational degrees of freedom of the knee joint:

$$\begin{aligned} \text{extension-flexion rotation} \quad & \theta_{EF} = \psi, \\ \text{varus-valgus rotation} \quad & \theta_{VV} = \theta, \\ \text{internal-external rotation} \quad & \theta_{IE} = \phi. \end{aligned}$$

It is well-accepted, see, for example, [9–11], that the extension-flexion (EF) axis is fixed to the femur and passes through its lateral and medial epicondyles, the internal-external rotation axis is fixed to the tibia and is parallel to its longitudinal axis, and the varus-valgus rotation axis is floating and is perpendicular to both the extension-flexion and internal-external rotation axes.

Commensurate with the choice of Euler angles, the basis $\{\mathbf{g}_1, \mathbf{g}_2, \mathbf{g}_3\}$ is defined, where the vector $\mathbf{g}_1 = \mathbf{p}_1$ is taken to be aligned with the femur-fixed extension-flexion axis, and the vector $\mathbf{g}_3 = \mathbf{d}_3$ is aligned with the tibia-fixed internal-external rotation axis (see Figures 2 and 3). A key feature of these axes is that the angle subtended by them is $\frac{\pi}{2}$ minus the varus-valgus rotation angle θ_{VV} (which is negative in Figure 3). The axis $\mathbf{g}_2$ associated with the latter angle of rotation points along the varus-valgus axis, which is both parallel to the tibial plateau and perpendicular to the line connecting the two points of contact between the femoral condyles and the tibial plateau.

Unlike the rotational axes of the knee joint, there is no universal agreement on the prescriptions for the axes of translation of the knee joint [1, 12]. For example, Grood and Suntay [1] use two sets of axes, one for "joint translations, which is equivalent to the set of rotation axes $\{\mathbf{g}_1, \mathbf{g}_2, \mathbf{g}_3\}$, and one for "clinical translations, which is equivalent to the dual of the rotation axes $\{\mathbf{g}^1, \mathbf{g}^2, \mathbf{g}^3\}$ (see Section 4.1 below for further details).

Here, we define a lateral-medial translation axis along the line connecting the two points of contact between the femoral condyles and tibial plateau, an anterior-posterior translation axis fixed to the tibia and parallel to the articular surface of the tibial plateau, and a compression-distraction

[3] In particular, expressions for, and graphical representations of, the Euler and dual Euler basis vectors for the 1-2-3 set of Euler angles are presented in (27) and in Figure 6.

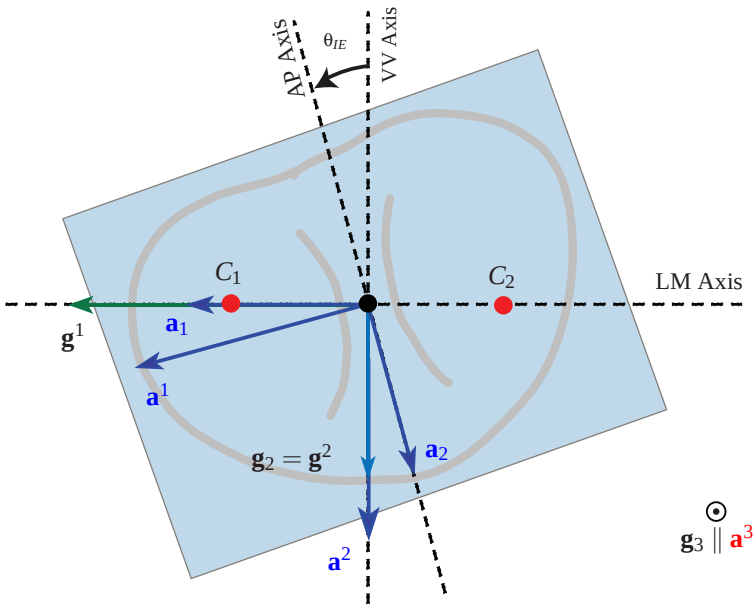

Fig. 2. Schematic of the transverse plane of the right knee joint. In the interests of clarity, the magnitudes of the vectors $\mathbf{a}^1$ and $\mathbf{a}^2$ have been exaggerated. The lateral-medial (LM), varus-valgus (VV), and anterior-posterior (AP) axes are also shown.

axis perpendicular to both the lateral medial and anterior-posterior translation axes. A basis $\{\mathbf{a}_1, \mathbf{a}_2, \mathbf{a}_3\}$ is defined with the help of the axes of translation (see Figures 2 and 3). In particular, we define $\mathbf{a}_1$ as a unit vector along the lateral-medial axis, $\mathbf{a}_2$ as a unit vector along the anterior-posterior axis of the tibia, and $\mathbf{a}_3$ as a unit vector in the compression-distraction direction:

$$\begin{aligned} \mathbf{a}_{LM} &= \mathbf{a}_1 = \cos(\theta_{VV})\,\mathbf{g}^1, \\ \mathbf{a}_{AP} &= \mathbf{a}_2 = \cos(\theta_{IE})\,\mathbf{g}_2 - \sin(\theta_{IE})\cos(\theta_{VV})\,\mathbf{g}^1, \\ \mathbf{a}_{CD} &= \mathbf{a}_3 = \mathbf{g}_3. \end{aligned} \tag{11}$$

The presence of $\cos(\theta_{VV})$ in the definitions $(11)_{1,2}$ is due to the fact that the magnitude of $\mathbf{g}^1$ is $\sec(\theta_{VV})$ The set of dual vectors $\{\mathbf{a}^1, \mathbf{a}^2, \mathbf{a}^3\}$ can be defined using (8) and (11):

$$\begin{aligned} \mathbf{a}^1 &= \cos(\theta_{VV})\,\mathbf{g}^1 + \tan(\theta_{IE})\,\mathbf{g}_2, \\ \mathbf{a}^2 &= \sec(\theta_{IE})\,\mathbf{g}_2, \\ \mathbf{a}^3 &= \mathbf{g}_3. \end{aligned} \tag{12}$$

Explicit representations for these basis vectors in terms of the basis vectors associated with the proximal and distal frames are presented in (32).

Given a displacement vector $\mathbf{d}$ of a point on the tibia relative to a point on the femur, we can write

$$\mathbf{d} = d^{LM}\mathbf{a}_1 + d^{AP}\mathbf{a}_2 + d^{CD}\mathbf{a}_3. \tag{13}$$

We take this opportunity to note that while the $\mathbf{a}_1$ and $\mathbf{a}_3$ are perpendicular, the same cannot be said for $\mathbf{a}_1$ and $\mathbf{a}_2$.Thus, a pure displacement $\mathbf{d} = d\mathbf{a}_1$ along the lateral-medial direction has scalar projections on both the lateral-medial ($\mathbf{d}\cdot\mathbf{a}_1 = d$) and anterior-posterior ($\mathbf{d}\cdot\mathbf{a}_2 = -d\sin(\theta_{IE})$) axes.

3.2 Representations of Forces and Moments

It is possible to represent the forces and moments acting on the knee joint using any of the seven sets of basis vectors discussed in Section 2.1. However the resulting representations are often inconvenient. For the forces and moments acting on the knee joint, of particular interest here are the representations

$$\begin{aligned} \mathbf{F} &= F_1\mathbf{a}^1 + F_2\mathbf{a}^2 + F_3\mathbf{a}^3, \\ \mathbf{M} &= M_1\mathbf{g}^1 + M_2\mathbf{g}^2 + M_3\mathbf{g}^3. \end{aligned} \tag{14}$$

The components M_k are computed by projecting $\mathbf{M}$ onto the Euler basis vectors: $M_k = \mathbf{M}\cdot\mathbf{g}_k$. Expressing force vectors and moment vectors as linear combinations of contravariant basis vectors and dual Euler basis vectors has a long and illustrious history. However, the basis vectors are often not

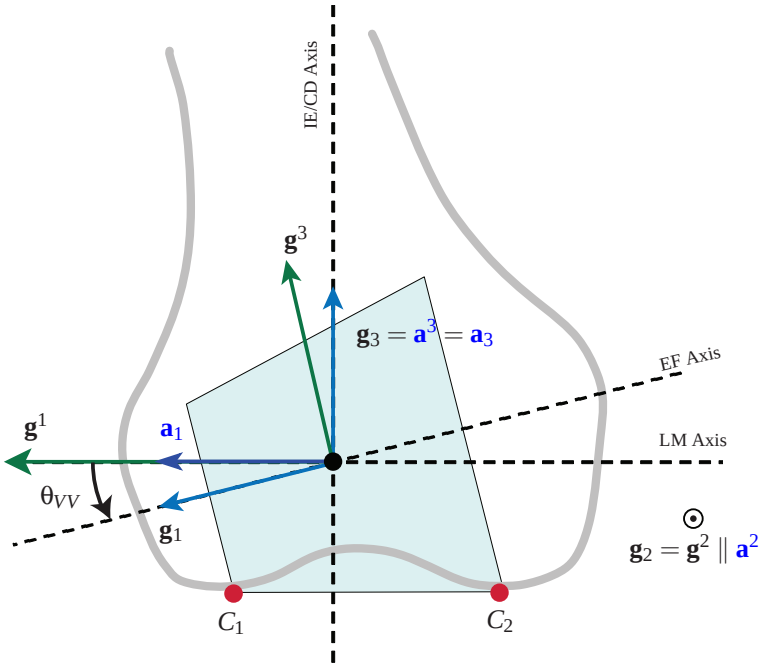

Fig. 3. Schematic of the frontal plane of the right knee joint. In this figure $\theta_{VV} < 0$, and the magnitudes of $\mathbf{g}^1$ and $\mathbf{g}^3$ have been exaggerated in the interests of clarity. The lateral-medial (LM), internal-external (IE), compression-distraction (CD), and anterior-posterior (AP) axes are also shown.

explicitly mentioned in classical texts and this can often be a source of confusion.

With the help of (31) or, equivalently, by computing $\mathbf{g}_i \cdot \mathbf{g}_k$, the relationship between the components M_k and M^i can be found:

$$\begin{bmatrix} M^1 \\ M^2 \\ M^3 \end{bmatrix} = \begin{bmatrix} \sec^2(\theta_{VV}) & 0 & -\frac{\sin(\theta_{VV})}{\cos^2(\theta_{VV})} \\ 0 & 1 & 0 \\ -\frac{\sin(\theta_{VV})}{\cos^2(\theta_{VV})} & 0 & \sec^2(\theta_{VV}) \end{bmatrix} \begin{bmatrix} M_1 \\ M_2 \\ M_3 \end{bmatrix},$$
$$\begin{bmatrix} M_1 \\ M_2 \\ M_3 \end{bmatrix} = \begin{bmatrix} 1 & 0 & \sin(\theta_{VV}) \\ 0 & 1 & 0 \\ \sin(\theta_{VV}) & 0 & 1 \end{bmatrix} \begin{bmatrix} M^1 \\ M^2 \\ M^3 \end{bmatrix}. \tag{15}$$

A key feature of these identities is the presence of θ_{VV}. For instance, as $|\theta_{VV}|$ increases from 0, then the components M_1 and M_3 become increasingly distinct from M^1 and M^3. Some examples of these relations are shown in Figure 4.

In a similar manner, the components $F_k = \mathbf{F} \cdot \mathbf{a}_k$ and $F^i = \mathbf{F} \cdot \mathbf{a}^i$ can be related with the help of (32):

$$\begin{bmatrix} F^1 \\ F^2 \\ F^3 \end{bmatrix} = \begin{bmatrix} \sec^2(\theta_{IE}) & \sec(\theta_{IE})\tan(\theta_{IE}) & 0 \\ \sec(\theta_{IE})\tan(\theta_{IE}) & \sec^2(\theta_{IE}) & 0 \\ 0 & 0 & 1 \end{bmatrix} \begin{bmatrix} F_1 \\ F_2 \\ F_3 \end{bmatrix},$$
$$\begin{bmatrix} F_1 \\ F_2 \\ F_3 \end{bmatrix} = \begin{bmatrix} 1 & -\sin(\theta_{IE}) & 0 \\ -\sin(\theta_{IE}) & 1 & 0 \\ 0 & 0 & 1 \end{bmatrix} \begin{bmatrix} F^1 \\ F^2 \\ F^3 \end{bmatrix}. \tag{16}$$

It is interesting to note the role played by the angle θ_{IE} representing internal-external rotation of the tibia in these relations: when the internal-external rotation is zero, then both sets of basis vectors and components are identical.

We next consider the power of an applied moment acting on the tibia. Assuming a fixed femur and given a relative motion of the tibia which has an angular velocity ω, then, with the help of (35), the power of an applied moment $\mathbf{M}_a = M_{a_1}\mathbf{g}^1 + M_{a_2}\mathbf{g}^2 + M_{a_3}\mathbf{g}^3$ has a simple representation:

$$\mathbf{M}_a \cdot \omega = M_{a_1}\dot{\theta}_{EF} + M_{a_2}\dot{\theta}_{VV} + M_{a_3}\dot{\theta}_{IE}. \tag{17}$$

The corresponding expression featuring the components M_a^k is far more complicated. Related remarks apply to an applied force $\mathbf{F}_a$.

3.3 Forces and Moments at the Condyles

A central feature of the knee joint are a pair of contact forces exerted by the condyles which prevents the tibial plateau from passing through them. These forces re-

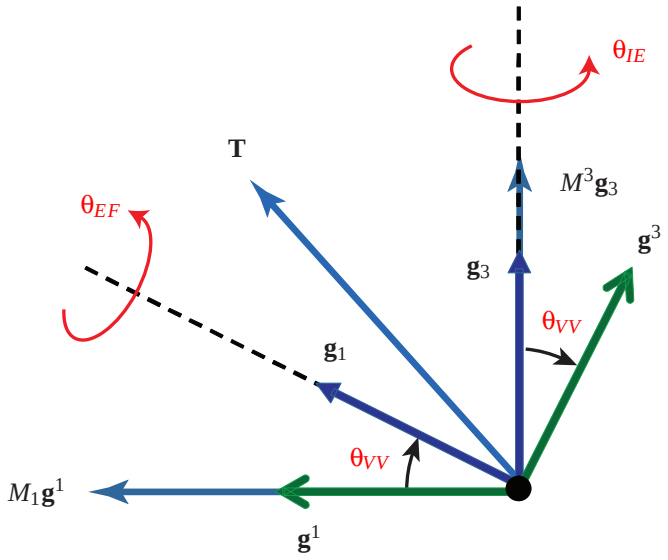

Fig. 4. Three representative examples of moments: $M^3\mathbf{g}_3$, $M_1\mathbf{g}^1 = M_1\sec^2(\theta_{VV})\mathbf{g}_1 - M_1\sec^2(\theta_{VV})\sin(\theta_{VV})\mathbf{g}_3$, and $\mathbf{T} = T^1\mathbf{g}_1 + T^3\mathbf{g}_3 = \left(T^1 + \sin(\theta_{VV})T^3\right)\mathbf{g}^1 + \left(T^3 + \sin(\theta_{VV})T^1\right)\mathbf{g}^3$. The different representations for the moments were obtained using (15).

strict varus-valgus rotation θ_{VV} and compression-distraction d^{CD}. Referring to Figures 3 and 5, the resultant of the pair of forces acts antiparallel to the $\mathbf{a}^3$ direction. The pair is equipollent to a resultant force $\mathbf{F}_c$ and a resultant moment $\mathbf{M}_c$ acting at point C:

$$\begin{aligned} \mathbf{F}_c &= \mu_1\mathbf{a}^3 = \mathbf{F}_{c_1} + \mathbf{F}_{c_2}, \\ \mathbf{M}_c &= \mu_2\mathbf{g}^2 = \pi_1 \times \mathbf{F}_{c_2} + \pi_2 \times \mathbf{F}_{c_2}. \end{aligned} \tag{18}$$

Here, π_1 and π_2 are the respective position vectors of the condyles C_1 and C_2 relative to C. The force $\mathbf{F}_c$ is an example of a constraint (or normal) force, while $\mathbf{M}_c$ is an example of a constraint moment. The latter serves to prevent rotation in the $\mathbf{g}_2$ direction. As the relative translational motion in the $\mathbf{a}_3$ and relative rotational motion in the $\mathbf{g}_2$ directions are assumed to be zero when both condyles are in contact with the tibia, $\mathbf{F}_c$ and $\mathbf{M}_c$ do no work.

3.4 Clinical Forces and Moments

Suppose a clinician wishes to test the soft tissue restraints against anterior translation by applying a force to the tibia. This force should lie entirely in the $\mathbf{a}^2$ direction. Otherwise, if $\theta_{IE} \neq 0$, the internal joint reaction force will have components that resist motions other than anterior translation. For example, if a clinician applies the external force $F_A\mathbf{a}_2$, then the opposing joint reaction force $(-F_A\mathbf{a}_2 = F_A\sin(\theta_{IE})\mathbf{a}^1 - F_A\mathbf{a}^2)$ will have a component $(F_A\sin(\theta_{IE})\mathbf{a}^1)$ that resists lateral translation in addition to a component $(-F_A\mathbf{a}^2)$ that resists anterior translation.

Similarly, to test the soft tissue restraints against internal rotation, a clinician should apply an external moment in the $\mathbf{g}^3$ direction. If instead, for example, a moment $M_A\mathbf{g}_3$ is applied, then the opposing joint reaction moment $(-M_A\mathbf{g}_3 = M_1\mathbf{g}^1 + M_3\mathbf{g}^3)$ will have a component $(M_1 = -M_A\sin(\theta_{VV})$ that resists flexion in addition to a component $(M_3 = -M_A)$ resisting internal rotation.

On the other hand, under an applied moment $M\mathbf{g}_2$, only a reaction moment in the $\mathbf{g}^2$ direction is required to prevent varus-valgus rotation, since $\mathbf{g}^2 = \mathbf{g}_2$ is perpendicular to the plane formed by the other basis vectors.

3.5 Infinitesimal Displacements and Rotations

For the purposes of understanding incremental displacements and rotations of the knee joint, we now consider the case where the knee joint has been given a finite displacement and rotation and an infinitesimal motion is then superposed on this motion. The finite rigid body motion is defined by the following displacements and angles:

$$d_0^{LM}, \qquad d_0^{AP}, \qquad d_0^{CD}, \qquad \theta_{EF0}, \qquad \theta_{VV0}, \qquad \theta_{IE0}. \tag{19}$$

The respective basis vectors associated with the given values of the angles and displacements are distinguished using subscript and superscript 0s.

The incremental rotation of the tibia relative to the femur

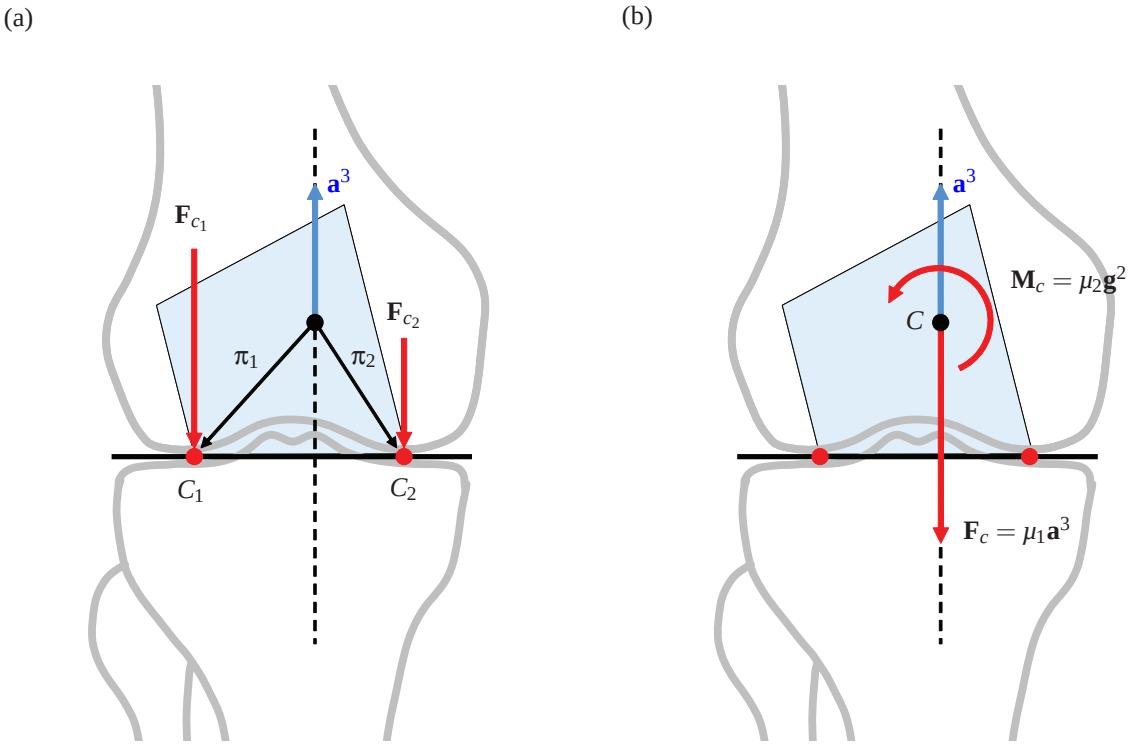

Fig. 5. The reaction forces $\mathbf{F}_{c_1}$ and $\mathbf{F}_{c_2}$ acting at the condyles shown in (a) are equipollent to a moment $\mathbf{M}_c = \pi_1 \times \mathbf{F}_{c_1} + \pi_2 \times \mathbf{F}_{c_2}$ and a force $\mathbf{F}_c = \mu_1 \mathbf{a}^3$ where $\mu_1 = (\mathbf{F}_{c_1} + \mathbf{F}_{c_2}) \cdot \mathbf{a}_3$ acting at the point C.

is defined by the vector $\delta\theta$ and incremental displacement of the tibia relative to the femur is defined by the vector $\delta\mathbf{d}$. These vectors have the respective representations:

$$\begin{aligned}\delta\theta &= \sum_{k=1}^{3} \delta\theta^i \mathbf{d}_i^0 = \delta\theta_{EF}\mathbf{g}_1^0 + \delta\theta_{VV}\mathbf{g}_2^0 + \delta\theta_{IE}\mathbf{g}_3^0,\\ \delta\mathbf{d} &= \sum_{k=1}^{3} \delta d_i \mathbf{d}_i^0 = \delta d^{LM}\mathbf{a}_1^0 + \delta d^{AP}\mathbf{a}_2^0 + \delta d^{CD}\mathbf{a}_3^0\\ &\quad + d_0^{LM}\delta\mathbf{a}_1 + d_0^{AP}\delta\mathbf{a}_2 + d_0^{CD}\delta\mathbf{a}_3. \quad (20)\end{aligned}$$

The increments $\delta\mathbf{a}_k$ are computed with the help of (11), (27) and (31). In addition, a Jacobian J can be defined:

$$\begin{bmatrix}\delta\theta^1\\ \delta\theta^2\\ \delta\theta^3\\ \delta d_1\\ \delta d_2\\ \delta d_3\end{bmatrix} = \mathsf{J}\begin{bmatrix}\delta\theta_{EF}\\ \delta\theta_{VV}\\ \delta\theta_{IE}\\ \delta d^{LM}\\ \delta d^{AP}\\ \delta d^{CD}\end{bmatrix}, \qquad \mathsf{J} = \begin{bmatrix}(\mathsf{E}_d)^T & 0\\ \mathsf{D} & (\mathsf{T}\mathsf{E}_d)^T\end{bmatrix}, \quad (21)$$

where the matrix D is a function of θ_{VV0}, θ_{EF0}, and θ_{IE0} and a linear function of d_0^{LM}, d_0^{CD}, and d_0^{AP} (see (36) in Appendix C). The Jacobian has an inverse

$$\mathsf{J}^{-1} = \begin{bmatrix}\mathsf{G}_d & 0\\ -(\mathsf{E}_d)^T\mathsf{T}^{-1}\mathsf{D}\mathsf{G}_d & \mathsf{G}_d\mathsf{T}^{-T}\end{bmatrix}. \quad (22)$$

The matrices G_d, T, and E_d in (21) and (22) are evaluated at θ_{VV0}, θ_{EF0}, and θ_{IE0}.

We emphasize that the Jacobian J presented here is related to, but distinct from, the Jacobian $\mathbf{J}_1$ discussed in [2]. There are two reasons for this. First, we use a different basis to describe the infinitesimal translations, and second we assume that all the components of $\mathbf{d}$ are not necessarily zero.

The Jacobian and its inverse can be used to infer how rotations and displacements about and along the tibial axes influence the Euler angles and the clinical displacements. For instance (21) and (22) can be used to show that an infinitesimal rotation $\delta\theta^1$ about $\mathbf{d}_1$ induces an infinitesimal extension-flexion $\delta\theta_{EF} = \sec(\theta_{VV0})\cos(\theta_{IE0})\,\delta\theta^1$, an infinitesimal varus-valgus rotation $\delta\theta_{VV} = \sin(\theta_{IE0})\,\delta\theta^1$, and an infinitesimal internal-external rotation $\delta\theta_{IE} = -\tan(\theta_{VV0})\cos(\theta_{IE0})\,\delta\theta^1$. Given the complexity of the 4th through 6th rows of J^{-1}, it is to be anticipated that an infinitesimal displacement δd^k will result in several infinitesi-

mal rotations (i.e., $\delta\theta_{EF}, \delta\theta_{VV}, \delta\theta_{IE}$) and infinitesimal clinical translations (i.e., $\delta d^{LM}, \delta d^{AP}, \delta d^{CD}$).

4 Discussion

As in [1], the femoral and tibial axes $\mathbf{g}_1$ and $\mathbf{g}_3$ can be defined using bony landmarks, and the axis $\mathbf{g}_2$ can then be defined as the unit vector perpendicular to the plane formed by $\mathbf{g}_1$ and $\mathbf{g}_3$. However, for a given motion, it is well-known that the choice of the femoral and tibial axes effects the resulting values of the three angles θ_{EF}, θ_{VV}, and θ_{IE} (see, e.g., [14]). To eliminate some of this variability, optimization schemes have been proposed with the aim of specifying $\mathbf{g}_1$ and/or $\mathbf{g}_3$ (see [15, 16] and references therein). These schemes seek to minimize some objective quantity (e.g., varus-valgus rotation and/or net tibial translation) under a particular set of assumptions (e.g., a compound pinned hinge model, or a shape function for the Euler angles) for a given motion of interest (e.g., flexion within the range of $40^\circ - 80^\circ$, or constrained tibial rotation). Motivated by the contact constraint force $\mathbf{F}_c$ and moment $\mathbf{M}_c$ described in Section 3.3, we suggest that an optimization scheme be chosen to minimize incremental varus-valgus rotations $\delta\theta_{VV}$ and compression-distraction translations δd^{CD}. Such an optimization scheme would be valid for any knee joint motion during which $\mathbf{F}_c$ and $\mathbf{M}_c$ do not perform work.

4.1 Forces and Moment Representations in Other Works

It is instructive to compare our work with earlier works on the kinematics and kinetics of the knee joint. Starting with work in [1], two distinct types of displacements are discussed: clinical displacements q_i and joint translations S_i. Using the dual Euler basis, it is straightforward to see that these displacements are simply related:[4]

$$q_1\mathbf{g}^1 + q_2\mathbf{g}^2 - q_3\mathbf{g}^3 = S_1\mathbf{g}_1 + S_2\mathbf{g}_2 + S_3\mathbf{g}_3. \tag{23}$$

Unfortunately, the magnitudes of $\mathbf{g}^1$ and $\mathbf{g}^3$ are $\sec(\theta_{VV})$ and so the magnitudes of the displacements q_1 and q_3 are difficult to interpret physically. Furthermore, since $\mathbf{g}^3$ is not perpendicular to the tibial plateau when $\theta_{VV} \neq 0$, natural joint translations would produce nonzero displacements q_3, which might be misinterpreted as unnatural joint compression or distraction. It was partially a result of these observations that we defined the unit vectors $\mathbf{a}_k$ for the clinical displacements d^{CD}, d^{LM}, and d^{AP}.

The seminal work on forces and moments at the knee joint is Fujie et al. [2]. In certain instances in this work, the forces and moments at the knee joint are expressed in terms of the $\mathbf{g}^k$ basis. Specifically, examining (10) and (11) in [2], one can interpret their components f_{LM}, f_{AP}, and f_{PD} as the force components $\mathbf{F}\cdot\mathbf{g}_k$, and their components m_{EF}, m_{VV}, and m_{IE} as the moment components $\mathbf{M}\cdot\mathbf{g}_k$, respectively. Here, $\mathbf{g}_k$ are the Euler basis vectors for a 3-1-2 set of Euler angles. That is,

$$\begin{aligned}\mathbf{M} &= m_{EF}\mathbf{g}^1 + m_{VV}\mathbf{g}^2 + m_{IE}\mathbf{g}^3,\\ \mathbf{F} &= f_{LM}\mathbf{g}^1 + f_{AP}\mathbf{g}^2 + f_{PD}\mathbf{g}^3.\end{aligned} \tag{24}$$

Thus, for example, m_{EF} is obtained by projecting $\mathbf{M}$ onto $\mathbf{g}_1 = \mathbf{p}_3$.

Unfortunately, Fujie et al. [2] did not explicitly mention the basis vectors they used when they described the aforementioned forces and moments which may cause confusion. For example, it was not clear that the "proximal-distal" force component f_{PD} acts in the $\mathbf{g}^3$ direction, which as mentioned earlier, is not necessarily perpendicular to the tibial plateau. Thus, $f_PD\mathbf{g}^3$ might be misinterpreted as a workless contact constraint force when in fact it would do work during natural joint translations. In this respect, Desroches et al. [13] deserve credit for pointing out the distinction between the components $\mathbf{M}\cdot\mathbf{g}_k$ and $\mathbf{M}\cdot\mathbf{g}^k$. Indeed by comparing $(14)_2$ to (1) in [13], we find that the joint coordinate system they are using is simply expressing the moment vector $\mathbf{M}$ as a linear combination of $\mathbf{g}_k$ with the components $\mathbf{M}\cdot\mathbf{g}^k$. However, these authors did not utilize results on dual Euler bases vectors as we do here.

4.2 Stiffness Matrices for the Knee Joint

Discussions of the stiffness of the knee joint can be found in the literature. For example, Cammarata and Dhaher [17] and Hsu et al. [18] present experimental measurements of the stiffness of the joint by comparing a varus-valgus rotation with the corresponding varus-valgus moment at 0° of flexion. Because of the multi-degree-of-freedom nature of the knee joint, this data constitutes one of the many components of the stiffness matrix of the knee joint and illuminates the difficulties in measuring a complete set of stiffness data for this joint.

To elaborate further, it is possible to construct a variety of stiffness matrices for the knee joint using the methods discussed in [3]. For instance, one such 6×6 matrix could relate the $\mathbf{E}_i$ components of the increments in $\mathbf{F}$ and $\mathbf{M}$ to the increments $\delta\theta_{EF}$, $\delta\theta_{VV}$, $\delta\theta_{IE}$, δd^{LM}, δd^{AP}, δd^{CD}. Alternatively, another stiffness matrix could be constructed relating the $\mathbf{d}_k$ components of the increments in $\mathbf{F}$ and $\mathbf{M}$ to the six increments $\delta\theta^j$ and δd^i. In the interests of brevity we don't present the explicit details here as they are easily

[4] See, in particular, equations (4c), (5a),..., (7) in [1]. In their work, $\mathbf{g}_i$ are denoted by $\mathbf{e}_i$ and a dual Euler basis is never mentioned.

inferred from [3]. However, one important point to note is that if the knee is loaded so that increments to compression-distraction and varus-valgus rotation are not possible (i.e., $\delta d^{CD} = 0$ and $\delta\theta_{VV} = 0$), then it is possible to construct a 4×4 stiffness matrix relating the increments in $\mathbf{F} \cdot \mathbf{a}_1$, $\mathbf{F} \cdot \mathbf{a}_2$, $\mathbf{M} \cdot \mathbf{g}_1$ and $\mathbf{M} \cdot \mathbf{g}_2$ to $\delta\theta_{EF}$, $\delta\theta_{IE}$, δd^{LM}, and δd^{AP}. Such a stiffness matrix would not be dominated by the components of the reaction force $F_3\mathbf{a}^3$ and the reaction moment $M_2\mathbf{g}^2$ which ensure that the compression-distraction and varus-valgus rotation remain constrained. This is a unique feature of the new coordinate system proposed in the present paper.

4.3 Closing Remarks

To summarize, we have introduced a coordinate system for describing knee joint kinematics and kinetics. Central to this coordinate system are two sets of basis vectors ($\{\mathbf{g}_1, \mathbf{g}_2, \mathbf{g}_3\}$ and $\{\mathbf{g}^1, \mathbf{g}^2, \mathbf{g}^3\}$) which are used to express joint rotations and joint moments in a manner consistent with [1, 2], and two analogous sets of basis vectors ($\{\mathbf{a}_1, \mathbf{a}_2, \mathbf{a}_3\}$ and $\{\mathbf{a}^1, \mathbf{a}^2, \mathbf{a}^3\}$) which are used to express joint translations and joint forces. All four sets of basis vectors are related by the Euler angles θ_{IE} and θ_{VV}. Importantly, since $\mathbf{a}_3 = \mathbf{a}^3$ and $\mathbf{g}_2 = \mathbf{g}^2$, our coordinate system highlights the articular contact force $F_c\mathbf{a}^3$ and moment $M_c\mathbf{g}^2$, which prevent incremental compression-distraction translations along $\mathbf{a}_3$ and varus-valgus rotations about $\mathbf{g}_2$, respectively. If aligned such that these incremental motions are minimal, our coordinate system simplifies the description of joint motions and also joint stiffnesses.

Achnowledgements

The work of MPS was supported by a National Science Foundation Graduate Research Fellowship.

References

[1] Grood, E. S., and Suntay, W. J., 1983. "A joint coordinate system for the clinical description of three-dimensional motions: Application to the knee". *Journal of Biomechanical Engineering*, **105**(2), pp. 136–144.

[2] Fujie, H., Livesay, G. A., Fujita, M., and Woo, S. L.-Y., 1996. "Forces and moment in six-DOF at the human knee joint: Mathematical description for control". *Journal of Biomechanics*, **29**(12), pp. 1577–1585.

[3] Metzger, M. F., Faruk Senan, N. A., and O'Reilly, O. M., 2010. "On Cartesian stiffness matrices in rigid body dynamics: An energetic perspective". *Multibody Syst. Dyn.*, **44**(4), pp. 441–472.

[4] O'Reilly, O. M., 2007. "The dual Euler basis: constraints, potentials, and Lagrange's equations in rigid body dynamics". *ASME Journal of Applied Mechanics*, **74**(2), pp. 1–10.

[5] O'Reilly, O. M., 2008. *Intermediate Dynamics for Engineers: A Unified Treatment of Newton-Euler and Lagrangian Mechanics*. Cambridge University Press, Cambridge.

[6] Howard, S., Žefran, M., and Kumar, V., 1998. "On the 6×6 Cartesian stiffness matrix for three-dimensional motions". *Mechanism and Machine Theory*, **33**(4), pp. 389–408.

[7] Žefran, M., and Kumar, V., 2002. "A geometrical approach to the study of the Cartesian stiffness matrix". *ASME Journal of Mechanical Design*, **124**(1), pp. 30–38.

[8] Simmonds, J. G., 1994. *A Brief on Tensor Analysis*, second ed. Springer-Verlag, New York.

[9] Churchill, D. L., Incavo, S. J., Johnson, C. C., and Beynnon, B. D., 1998. "The transepicondylar axis approximates the optimal flexion axis of the knee". *Clinical Orthopaedics and Related Research*, **356**, pp. 111–118.

[10] Hollister, A. M., Jatana, S., Singh, A. K., Sullivan, W. W., and Lupichuk, A. G., 1993. "Rotation of the knee". *Clinical Orthopaedics and Related Research*, **290**, pp. 159–268.

[11] Asano, T., Akagi, M., and Nakamura, T., 2005. "Ithe functional flexion-extension axis of the knee corresponds to the surgical epicondylar axis: In vivo analysis using a biplanar image-matching technique". *The Journal of Arthroplasty*, **20**(8), pp. 1060–1067.

[12] Bull, A. M. J., and Amis, A. A., 1998. "Knee joint motion: Description and measurement". *Proceedings of the Institution of Mechanical Engineers, Part H: Journal of Engineering in Medicine*, **212**(5), pp. 357–372.

[13] Desroches, G., Chèze, L., and Dumas, R., 2010. "Expression of joint moment in the joint coordinate system". *Journal of Biomechanical Engineering*, **132**(11), p. 114503.

[14] Most, E., Axe, J., Rubash, H., and Li, G., 2004. "Sensitivity of the knee joint kinematics calculation to selection of flexion axes". *Journal of Biomechanics*, **37**(11), pp. 1743 – 1748.

[15] Ehrig, R. M., Taylor, W. R., Duda, G. N., and Heller, M. O., 2007. "A survey of formal methods for determining functional joint axes". *Journal of Biomechanics*, **40**(10), pp. 2150–2157.

[16] Reichl, I., Auzinger, W., Schmiedmayer, H.-B., and Weinmüller, E., 2010. "Reconstructing the knee joint mechanism from kinematic data". *Mathematical and Computer Modelling of Dynamical Systems*, **16**(5),

pp. 403–415.
[17] Cammarata, M. L., and Dhaher, Y. Y., 2008. "The differential effects of gender, anthropometry, and prior hormonal state on frontal plane knee joint stiffness". *Clinical Biomechanics*, **23**(7), pp. 937 – 945.
[18] Hsu, W.-H., Fisk, J. A., Yamamoto, Y., Debski, R. E., and Woo, S. L.-Y., 2006. "Differences in torsional joint stiffness of the knee between genders". *The American Journal of Sports Medicine*, **34**(5), pp. 765–770.

Appendix A: Explicit expressions for the Euler and dual Euler basis vectors for the 1-2-3 set of Euler angles

In the paper, we follow [1] and use a 1-2-3 set of Euler angles. For the 1-2-3 set, the rotation R has the decomposition

$$\mathsf{R} = \mathsf{CBA}, \tag{25}$$

where A, B, and C are three rotation matrices:

$$\begin{aligned}
\mathsf{A} &= \begin{bmatrix} 1 & 0 & 0 \\ 0 & \cos(\psi) & \sin(\psi) \\ 0 & -\sin(\psi) & \cos(\psi) \end{bmatrix}, \\
\mathsf{B} &= \begin{bmatrix} \cos(\theta) & 0 & -\sin(\theta) \\ 0 & 1 & 0 \\ \sin(\theta) & 0 & \cos(\theta) \end{bmatrix}, \\
\mathsf{C} &= \begin{bmatrix} \cos(\phi) & \sin(\phi) & 0 \\ -\sin(\phi) & \cos(\phi) & 0 \\ 0 & 0 & 1 \end{bmatrix}.
\end{aligned} \tag{26}$$

The most frequently used choice of Euler angles in biomechanics is the 3-2-1 set and the corresponding developments for this set can be found in [4, 5].

The Euler basis and dual Euler basis for the 1-2-3 set of Euler angles can be expressed in terms of the proximal basis vectors and the distal basis vectors:

$$\begin{aligned}
\begin{bmatrix} \mathbf{g}_1 \\ \mathbf{g}_2 \\ \mathbf{g}_3 \end{bmatrix} &= \mathsf{E}_p \begin{bmatrix} \mathbf{p}_1 \\ \mathbf{p}_2 \\ \mathbf{p}_3 \end{bmatrix} = \mathsf{E}_d \begin{bmatrix} \mathbf{d}_1 \\ \mathbf{d}_2 \\ \mathbf{d}_3 \end{bmatrix}, \\
\begin{bmatrix} \mathbf{g}^1 \\ \mathbf{g}^2 \\ \mathbf{g}^3 \end{bmatrix} &= \mathsf{G}_p \begin{bmatrix} \mathbf{p}_1 \\ \mathbf{p}_2 \\ \mathbf{p}_3 \end{bmatrix} = \mathsf{G}_d \begin{bmatrix} \mathbf{d}_1 \\ \mathbf{d}_2 \\ \mathbf{d}_3 \end{bmatrix}.
\end{aligned} \tag{27}$$

The four matrices in these equations have the representations

$$\mathsf{E}_p = \begin{bmatrix} 1 & 0 & 0 \\ 0 & \cos(\psi) & \sin(\psi) \\ \sin(\theta) & -\cos(\theta)\sin(\psi) & \cos(\theta)\cos(\psi) \end{bmatrix},$$

$$\mathsf{E}_d = \begin{bmatrix} \cos(\theta)\cos(\phi) & -\cos(\theta)\sin(\phi) & \sin(\theta) \\ \sin(\phi) & \cos(\phi) & 0 \\ 0 & 0 & 1 \end{bmatrix}, \tag{28}$$

and

$$\begin{aligned}
\mathsf{G}_p &= \begin{bmatrix} 1 & \sin(\psi)\tan(\theta) & -\cos(\psi)\tan(\theta) \\ 0 & \cos(\psi) & \sin(\psi) \\ 0 & -\sec(\theta)\sin(\psi) & \sec(\theta)\cos(\psi) \end{bmatrix}, \\
\mathsf{G}_d &= \begin{bmatrix} \sec(\theta)\cos(\phi) & \sec(\theta)\sin(\phi) & 0 \\ \sin(\phi) & \cos(\phi) & 0 \\ -\tan(\theta)\cos(\phi) & \tan(\theta)\sin(\phi) & 1 \end{bmatrix}.
\end{aligned} \tag{29}$$

The second Euler angle needs to be restricted to $\theta \in \left(-\frac{\pi}{2}, \frac{\pi}{2}\right)$. We also note the identities:

$$\mathsf{E}_d = \mathsf{E}_p\mathsf{R}, \qquad \mathsf{G}_d\left(\mathsf{E}_d\right)^{-1} = \mathsf{G}_p\left(\mathsf{E}_p\right)^{-1},$$

$$\mathsf{G}_d = \left(\mathsf{E}_d\right)^{-T} = \mathsf{G}_p\mathsf{R}^T, \qquad \mathsf{G}_p = \left(\mathsf{E}_p\right)^{-T} = \mathsf{G}_d\mathsf{R}. \tag{30}$$

These identities can be used to establish the following relationships:

$$\begin{aligned}
\begin{bmatrix} \mathbf{g}^1 \\ \mathbf{g}^2 \\ \mathbf{g}^3 \end{bmatrix} &= \sec^2(\theta) \begin{bmatrix} 1 & 0 & -\sin(\theta) \\ 0 & \cos^2(\theta) & 0 \\ -\sin(\theta) & 0 & 1 \end{bmatrix} \begin{bmatrix} \mathbf{g}_1 \\ \mathbf{g}_2 \\ \mathbf{g}_3 \end{bmatrix}, \\
\begin{bmatrix} \mathbf{g}_1 \\ \mathbf{g}_2 \\ \mathbf{g}_3 \end{bmatrix} &= \begin{bmatrix} 1 & 0 & \sin(\theta) \\ 0 & 1 & 0 \\ \sin(\theta) & 0 & 1 \end{bmatrix} \begin{bmatrix} \mathbf{g}^1 \\ \mathbf{g}^2 \\ \mathbf{g}^3 \end{bmatrix}.
\end{aligned} \tag{31}$$

To illuminate the relations (27), it is convenient to consider graphical representations of the various basis vectors. These representations, first with respect to the distal basis, and then with respect to the proximal basis are shown in Figure 6, respectively. Referring to Figure 6, we observe a pair of cones of semi-angle θ whose axes of symmetry are defined by $\mathbf{g}_1$ and $\mathbf{g}_3$, respectively. For a fixed value of θ the cones can be considered to spin (ψ) and precess (ϕ).

With the help of (27) and (31), we can express (11) and (12) in several convenient representations:

$$\begin{aligned}
\begin{bmatrix} \mathbf{a}_1 \\ \mathbf{a}_2 \\ \mathbf{a}_3 \end{bmatrix} &= \mathsf{T}\mathsf{E}_p \begin{bmatrix} \mathbf{p}_1 \\ \mathbf{p}_2 \\ \mathbf{p}_3 \end{bmatrix} = \mathsf{T}\mathsf{E}_d \begin{bmatrix} \mathbf{d}_1 \\ \mathbf{d}_2 \\ \mathbf{d}_3 \end{bmatrix} \\
&= \begin{bmatrix} 1 & -\sin(\phi) & 0 \\ -\sin(\phi) & 1 & 0 \\ 0 & 0 & 1 \end{bmatrix} \begin{bmatrix} \mathbf{a}^1 \\ \mathbf{a}^2 \\ \mathbf{a}^3 \end{bmatrix},
\end{aligned}$$

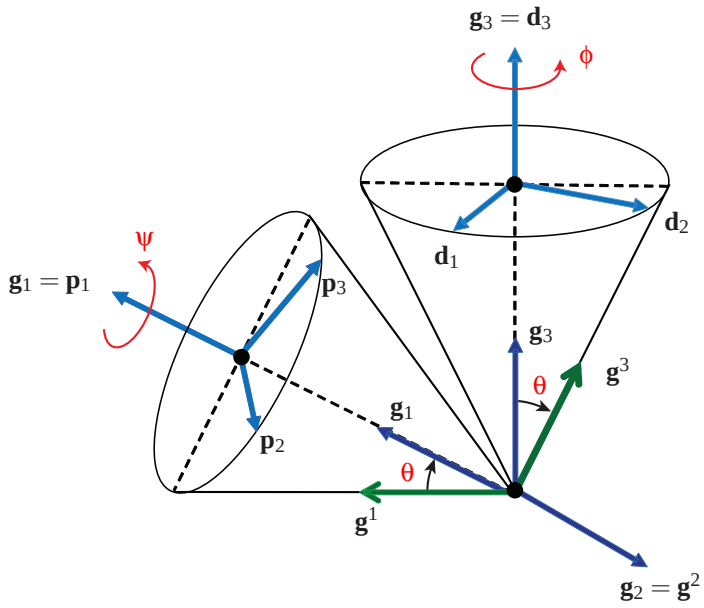

Fig. 6. Graphical representation of the dual Euler and Euler basis vectors and their relationships with the proximal $\mathbb{P}$ and distal $\mathbb{D}$ frames. Explicit expressions for these vectors can be found in (27). In this figure $\theta > 0$.

$$\begin{bmatrix} \mathbf{a}^1 \\ \mathbf{a}^2 \\ \mathbf{a}^3 \end{bmatrix} = \mathsf{T}^{-T}\mathsf{G}_p \begin{bmatrix} \mathbf{p}_1 \\ \mathbf{p}_2 \\ \mathbf{p}_3 \end{bmatrix} = \mathsf{T}^{-T}\mathsf{G}_d \begin{bmatrix} \mathbf{d}_1 \\ \mathbf{d}_2 \\ \mathbf{d}_3 \end{bmatrix} = \begin{bmatrix} \sec^2(\phi) & \sec(\phi)\tan(\phi) & 0 \\ \sec(\phi)\tan(\phi) & \sec^2(\phi) & 0 \\ 0 & 0 & 1 \end{bmatrix} \begin{bmatrix} \mathbf{a}_1 \\ \mathbf{a}_2 \\ \mathbf{a}_3 \end{bmatrix}. \quad (32)$$

Here, the matrix T and its inverse T^{-1} are

$$\mathsf{T} = \begin{bmatrix} \sec(\theta) & 0 & -\tan(\theta) \\ -\sin(\phi)\sec(\theta) & \cos(\phi) & \sin(\phi)\tan(\theta) \\ 0 & 0 & 1 \end{bmatrix},$$
$$\mathsf{T}^{-1} = \begin{bmatrix} \cos(\theta) & 0 & \sin(\theta) \\ \tan(\phi) & \sec(\phi) & 0 \\ 0 & 0 & 1 \end{bmatrix}. \quad (33)$$

Appendix B: Angular Velocity and Displacements

The angular velocity vector ω associated with the 1-2-3 Euler angles has several equivalent representations

$$\begin{aligned} \omega &= \dot{\psi}\mathbf{g}_1 + \dot{\theta}\mathbf{g}_2 + \dot{\phi}\mathbf{g}_3 \\ &= \omega_1\mathbf{d}_1 + \omega_2\mathbf{d}_2 + \omega_3\mathbf{d}_3 \\ &= \Omega_1\mathbf{p}_1 + \Omega_2\mathbf{p}_2 + \Omega_3\mathbf{p}_3. \end{aligned} \quad (34)$$

Using (27), it follows that

$$\begin{bmatrix} \omega_1 \\ \omega_2 \\ \omega_3 \end{bmatrix} = (\mathsf{E}_d)^T \begin{bmatrix} \dot{\psi} \\ \dot{\theta} \\ \dot{\phi} \end{bmatrix}, \qquad \begin{bmatrix} \omega_1 \\ \omega_2 \\ \omega_3 \end{bmatrix} = \mathsf{R} \begin{bmatrix} \Omega_1 \\ \Omega_2 \\ \Omega_3 \end{bmatrix}. \quad (35)$$

These results are used to relate incremental rotations of the tibia (ω_i) and femur (Ω_i) to changes in the Euler angles and vice versa.

Appendix C: An Element of the Jacobian

For completeness, the lengthy expression for the matrix D appearing in the expressions (21) and (22) for the Jacobian and its inverse is given in this Appendix. Explicitly,

$$\mathsf{D} = d_0^{LM}\mathsf{D}_1 + d_0^{AP}\mathsf{D}_2 + d_0^{CD}\mathsf{D}_3, \quad (36)$$

where

$$\mathsf{D}_1 = \begin{bmatrix} \sin(\theta_{VV})\sin(\theta_{IE}) & -\tan(\theta_{VV})\cos(\theta_{IE}) & 0 \\ \sin(\theta_{VV})\cos(\theta_{IE}) & -\tan(\theta_{VV})\sin(\theta_{IE}) & 0 \\ 0 & \tan(\theta_{VV})\left(\tan(\theta_{VV}) - \sec(\theta_{VV})\right) & 0 \end{bmatrix},$$

$$\mathsf{D}_2 = \begin{bmatrix} 0 & -\sin(\theta_{IE})\cos(\theta_{IE})\tan(\theta_{VV}) & -\cos(2\theta_{IE}) \\ 0 & -\sin^2(\theta_{IE})\tan(\theta_{VV}) & 0 \\ 0 & 0 & 0 \end{bmatrix}$$

$$
- \begin{bmatrix} \sin(\theta_{VV})\sin^2(\theta_{IE}) & 0 & 0 \\ \sin(\theta_{VV})\sin(\theta_{IE})\cos(\theta_{IE}) & 0 & 0 \\ 0 & x & 0 \end{bmatrix}
$$

$$
+ \begin{bmatrix} \sin(\theta_{VV})\cos(\theta_{VV})\cos(\theta_{IE}) & 0 & 2\cos(\theta_{VV})\cos(\theta_{IE}) \\ \sin(\theta_{VV})\sin(\theta_{IE})\cos(\theta_{VV}) & 0 & 0 \\ \cos^2(\theta_{VV}) & 0 & 0 \end{bmatrix},
$$

$$
\mathsf{D}_3 = \begin{bmatrix} -\cos(\theta_{VV})\sin(\theta_{IE}) & \cos(\theta_{IE}) & 0 \\ -\cos(\theta_{VV})\cos(\theta_{IE}) & -\sin(\theta_{IE}) & 0 \\ 0 & 0 & 0 \end{bmatrix}. \tag{37}
$$

In the expression for D_2,

$$
x = -\sin(\theta_{VV})\sin(\theta_{IE})\sec^2(\theta_{VV}) + \sin(\theta_{IE})\tan^2(\theta_{VV}). \tag{38}
$$

For convenience, we have dropped the superscript 0 appearing on θ_{VV}, θ_{EF}, and θ_{IE}.